



Open Access

ORIGINAL ARTICLE

Erectile Dysfunction

Vacuum therapy ameliorates erectile dysfunction in bilateral cavernous nerve crush rats by inhibiting apoptosis and activating autophagy

Chang-Jing Wu^{1,*}, Fu-Dong Fu^{1,2,*}, Feng Qin¹, Ming Ma^{1,3}, Tao Li^{1,3}, Shan-Zun Wei^{1,3}, Bo-Tao Yu^{1,3}, Xin-Zong Yang¹, Jiu-Hong Yuan^{1,3}

Postprostatectomy erectile dysfunction (pPED) remains a current problem despite improvements in surgical techniques. Vacuum therapy is clinically confirmed as a type of pPED rehabilitation. However, its underlying mechanisms are incompletely understood. Recently, autophagy and apoptosis were extensively studied in erectile dysfunction resulting from diabetes, senescence, and androgen deprivation but not in the context of pPED and vacuum therapy. Therefore, this study was designed to investigate the roles of autophagy and apoptosis in pPED and vacuum therapy. Twenty-four adult male Sprague–Dawley rats were randomly divided into three groups: the control group, bilateral cavernous nerve crush (BCNC) group, and BCNC + vacuum group. After 4 weeks of treatment, intracavernosal pressure was used to evaluate erectile function. Real-time quantitative polymerase chain reaction, western blot, and immunohistochemistry were used to measure the molecular expression. TdT-mediated dUTP nick-end labeling staining was used to assess apoptosis. Transmission electron microscopy was used to observe autophagosomes. After treatment, compared with those of the BCNC group, erectile function and cavernosal hypoxia had statistically significantly improved ($P < 0.05$). Apoptosis and the relative protein expression of B-cell lymphoma-2-associated X and cleaved Caspase3 were decreased ($P < 0.05$). Autophagy-related molecules such as phosphorylated unc-51-like autophagy-activating kinase 1 (Ser757) and p62 were decreased. Beclin1, microtubule-associated protein 1 light chain 3 A/B, and autophagosomes were increased ($P < 0.05$). Besides, the phosphatidylinositol 3-kinase/AKT/mammalian target of rapamycin signaling pathway, as a negative regulator of autophagy to some degree, was inhibited. This study revealed that vacuum therapy ameliorated pPED in BCNC rats by inhibiting apoptosis and activating autophagy.

Asian Journal of Andrology (2021) 23, 273–280; doi: 10.4103/aja.aja_79_20; published online: 15 January 2021

Keywords: apoptosis; autophagy; bilateral cavernous nerve crush; erectile dysfunction; vacuum therapy

INTRODUCTION

Radical prostatectomy (RP) remains the gold standard for clinically localized prostate cancer, but urinary incontinence and erectile dysfunction are other challenges associated with RP.^{1,2} With the application of laparoscopic and robotic techniques, the incidence of urinary incontinence has dramatically decreased; however, approximately 14%–90% of patients still suffer postprostatectomy erectile dysfunction (pPED).³ To improve the quality of life of patients and their spouses, various strategies have been used for penile rehabilitation. Phosphodiesterase type 5 inhibitors (PDE5Is) have achieved great acceptance. However, some practices found that orally administered selective PDE5Is were disappointing in pPED patients.^{4,5} In addition, intracavernosal injections of prostaglandin E₁ or intraurethral suppositories have also been shown to be helpful for penile rehabilitation, but painful injections and unpleasant erections lead to poor patient compliance.^{6,7} Many years ago, vacuum therapy had already been recommended for penile rehabilitation. Currently,

the effects of vacuum therapy on pPED have been clinically confirmed; for example, the early use of vacuum therapy for pPED not only has the potential to restore spontaneous erections but it can also maintain penile length and increase penile hardness.^{8–10} However, the underlying molecular mechanisms are still incompletely understood.

Many studies have demonstrated that pPED results from unavoidable cavernous nerve injury after RP, which subsequently leads to the loss of spontaneous erection and the absence of cavernosal oxygenation.¹¹ Therefore, some researchers hypothesized that vacuum therapy exerted its effects through the nitric oxide/cyclic guanosine monophosphate (NO/cGMP) signaling pathway to mediate corporal smooth muscle relaxation.^{12,13} In addition, cavernous nerves are the main erection nerves and can regulate a variety of downstream cells, such as corpus cavernosum smooth muscle cells, endothelial cells, and mesenchymal cells.¹⁴ Previous studies showed that cavernous nerve damage could induce cavernosum smooth muscle cell apoptosis; furthermore, the reduction in smooth muscle cells resulted in

¹Andrology Laboratory, West China Hospital, Sichuan University, Chengdu 610041, China; ²Institutes for Systems Genetics, West China Hospital, Sichuan University, Chengdu 610041, China; ³Department of Urology, West China Hospital, Sichuan University, Chengdu 610041, China.

*These authors contributed equally to this work.

Correspondence: Dr. JH Yuan (jiuhongyuan2107@163.com)

Received: 13 May 2020; Accepted: 26 October 2020

veno-occlusive dysfunction and pPED.^{15–17} An increasing number of studies showed that vacuum therapy could preserve erectile function and penile length in bilateral cavernous nerve crush (BCNC) rats via antihypoxic, antiapoptotic, and antifibrotic mechanisms.¹¹

Autophagy and apoptosis play crucial roles in maintaining intracellular homeostasis. When cells suffer prolonged nutrient deprivation, oxidative stress, and aging, autophagy and apoptosis are successively activated.^{18,19} In general, mild autophagy protects cells from death, whereas severe and rapid autophagy always induces cell death.²⁰ Recently, an increasing number of studies have demonstrated that autophagy is involved in erectile dysfunction caused by diabetes mellitus, senescence, and androgen deprivation.^{21–23} Regulating the levels of autophagy and apoptosis through various therapies helped improve erectile function.^{24,25} However, currently, no data have been found on the roles of autophagy in pPED and vacuum therapy. Therefore, this study was designed to investigate whether autophagy plays a role in vacuum therapy-mediated effects on pPED.

MATERIALS AND METHODS

Animals

All the animal experiments in this study were approved by the Animal Care and Animal Ethics Committee of West China Hospital, Sichuan University, Chengdu, China (No. 2017057A). Twenty-four male Sprague–Dawley rats (10 weeks old, 280–330 g) were purchased from Chengdu Dossy Experimental Animals Co., Ltd. (Chengdu, China) for this study. After 3 days of adaptive feeding, the rats were randomly and equally divided into three groups: the control group (cavernous nerve exposure surgery only), BCNC group (BCNC surgery), and BCNC + vacuum group (BCNC surgery plus vacuum therapy). The vacuum erection device was purchased from Chengdu Xin Wei Cheng Technology Co., Ltd. (Chengdu, China). BCNC surgery was performed as described in our previous study.²⁶ In short, the rats were anesthetized, and then an ultrafine hemostat (12.5 cm, nonserrated; RWD Life Science, Shenzhen, China) was utilized to crush the cavernous nerves at a location 5 mm distal to the ganglion, with full tip closure for 30 s, removal for 30 s, and further closure for 30 s. In this study, the recommended vacuum pressure (–200 mmHg) was selected, and therapy started at 1 week after BCNC surgery; treatment was administered for 5 min twice daily with a 2-min interval from Monday to Friday and lasted for 4 weeks.²⁷ Subsequently, the rats were sacrificed for further analysis.

In vivo erectile function assay

As in previous studies, the intracavernosal pressure (ICP), maximal ICP/mean arterial pressure (max ICP/MAP) ratio, and area under the curve (AUC) of ICP upon cavernous nerve electrostimulation were used to evaluate erectile function in each group.^{11,26} After the functional experiments, all of the penile tissues were harvested for histological staining and molecular examination.

Real-time quantitative polymerase chain reaction (RT-qPCR)

Total RNA of the corpus cavernosum was isolated using TRNzol Universal (DP424, TIANGEN, Beijing, China) and reverse transcribed to cDNA with a FastQuant RT kit with gDNase (KR106, TIANGEN). Then, RT-qPCR was performed using 2× TSINGKE Master qPCR Mix SYBR Green I (TSE201, TSINGKE, Beijing, China). All the procedures were strictly performed according to the kit instructions. The level of *β-actin* messenger RNA (mRNA) was used to standardize the target genes, and the relative quantification of PCR products was calculated using the $2^{-\Delta\Delta CT}$ method. The associated gene primer sequences are shown in **Supplementary Table 1**.

Western blot (WB) analysis

Penile tissues were cut and homogenized in the radioimmunoprecipitation assay (RIPA) lysis buffer (MA0151, Meilunbio, Dalian, China) containing a protease inhibitor and phosphatase inhibitor cocktail (Millipore Corporation, Billerica, MA, USA). Protein concentrations were subsequently determined by a Pierce BCA protein assay kit (23227, Thermo Fisher Scientific Inc., Waltham, MA, USA), and bovine serum albumin was used as a standard. After adjustments, equal amounts (40 μg per lane) of protein were separated by 10% and 12% sodium dodecyl sulfate polyacrylamide gel electrophoresis (BAIHE Science and Technology, Chengdu, China) and transferred to polyvinylidene fluoride membranes (Millipore Corporation). Nonfat milk (5%) was used to block nonspecific binding sites. Then, the membranes were incubated overnight at 4°C with primary antibodies, the related information of which is listed in **Supplementary Table 2**. The next day, the membranes were incubated with anti-rabbit or anti-mouse secondary antibodies. Finally, Immobilon Western Chemiluminescent Substrate (WBKLS0500, Millipore Corporation) was used to visualize the proteins. The images were captured using the ChemiDoc MP imaging system (Bio-Rad Laboratories, Inc., Hercules, CA, USA), and the relative quantification of each protein to β -actin was performed using ImageJ 1.46r (National Institutes of Health, Wayne Rasband, MD, USA).

Histological studies

The middle part of the penis was selected for histological studies. After these tissues were rinsed using phosphate-buffered solution and fixed in 4.0% paraformaldehyde overnight, they were delivered to the pathological laboratory of West China Hospital (Sichuan University) for standard processing, such as dehydration, embedding, and sectioning. The penile tissues were cut into 5-μm sections for further immunohistochemical and apoptosis staining.

Immunohistochemistry (IHC)

IHC was performed by the streptavidin-peroxidase method by strictly following the manufacturer's instructions (SP-9000, Beijing ZSbio, Beijing, China). Briefly, 3% hydrogen peroxide was used to eliminate intracellular catalase. Normal horse serum (10%) was used to block nonspecific binding sites. Then, the samples were incubated with primary antibodies as listed in **Supplementary Table 2** overnight at 4°C. Meanwhile, the negative control was incubated with normal serum from the host species instead of primary antibodies. The next day, after being rinsed with phosphate buffer, the samples were incubated with anti-rabbit or anti-mouse IgG-conjugated biotin and further incubated with streptavidin-conjugated horseradish peroxidase. Finally, the samples were reacted with 3,3'-diaminobenzidine (DAB; ZLI-9018, Beijing ZSbio) to visualize the positive signal (brown) and stained with hematoxylin to visualize the cell nuclei. Then, the samples were imaged under ×100, ×200, and ×400 magnifications by a Zeiss Ax10 Imager (ZEISS, Oberkochen, Germany) and qualified using Image-Pro Plus version 6.0 (Media Cybernetics, Inc., Rockville, MD, USA). Three sections from each rat were analyzed, and there were five rats per group.

Apoptosis evaluation

The DeadEnd Fluorometric TUNEL System (G3250, Promega, Madison, WI, USA) was used for apoptosis evaluation and was strictly performed following the manufacturer's instructions. Apoptotic cells in the cavernosum were marked by green fluorescein, and all cell nuclei were stained with 4',6'-diamidino-2-phenylindole (DAPI; C0065, Solarbio, Beijing, China) and marked by blue fluorescein. The ratios of the percentage of apoptotic cells to total cells in each group of rats ($n = 5$) were recorded as the apoptosis index.

Electron microscopy

Freshly dissected cavernosum tissues were carefully cut into 1-mm³ sections and fixed in 3% glutaraldehyde overnight at 4°C. Then, the samples were sent to Chengdu LILAI Biotechnology Co. (Chengdu, China) for further dehydration, embedding, and sectioning. The samples were adhered to copper grids and imaged using an H-600IV transmission electron microscope (TEM; Hitachi group, Tokyo, Japan). Observations of subcellular structures, such as mitochondria, the endoplasmic reticulum, and autophagosomes, were used to assess cell damage and autophagy levels.

Statistical analyses

All data were expressed as the mean ± standard deviation. Related analyses and statistical charts were obtained using GraphPad Prism 5.0 software (GraphPad Software, San Diego, CA, USA). One-way analysis of variance followed by a Tukey test was used to analyze the differences between the three groups. Student's *t*-test was used to evaluate the difference between two groups. *P* < 0.05 was considered statistically significant.

RESULTS

Vacuum therapy improved erectile dysfunction

In this study, cavernous nerve electrostimulation at 5 V for 50 s was performed to evaluate erectile function. The ICP, max ICP/MAP, and AUC of the three groups were used to analyze the erection ability. Compared with those of the BCNC group, the values of ICP, max ICP/MAP, and AUC in the vacuum therapy group had statistically significantly increased (all *P* < 0.05). However, compared to those of the control group, the results of the vacuum therapy group suggested that only partial recovery was obtained (*P* < 0.05; **Figure 1**).

Vacuum therapy increased cavernosal oxygenation

The underlying pathological mechanisms of pPED are described in the introduction section. Therefore, some molecules, such as neuronal nitric oxide synthesis (nNOS), endothelial nitric oxide synthase (eNOS), and hypoxia-inducible factor-1α (HIF-1α), which are closely related to cavernosal oxygenation, were measured. RT-qPCR, WB,

and IHC results showed that compared with that of the BCNC group, the protein expression of HIF-1α in the vacuum therapy group had significantly decreased (*P* < 0.05), but not in the control group. Similar to the findings of previous studies, under normal oxygen conditions, the intracellular protein level of HIF-1α was dependent on its ubiquitination-mediated degradation rather than its transcriptional level.²⁸ It was these consequences that explained the RT-qPCR results in which no significant differences were found (*P*=0.46) among the control group, BCNC group, and vacuum therapy group. For eNOS and nNOS, the protein measurement results were consistent with the mRNA quantifications. The expression of eNOS and nNOS in the BCNC group was much lower than that in the control group (both *P* < 0.05). However, after one month of therapy, eNOS and nNOS had significantly upregulated (both *P* < 0.05). These data suggested that vacuum therapy improved pPED by increasing cavernosal oxygenation (**Figure 2**).

Vacuum therapy inhibited apoptosis

TdT-mediated dUTP nick-end labeling staining labeled apoptotic cells with green fluorescein, and DAPI marked cell nuclei with blue fluorescein. The ratio of apoptotic to total cells in the BCNC group had increased significantly in comparison with that of the control group, *P* < 0.05. However, after vacuum therapy, apoptosis had significantly inhibited (*P* < 0.05; **Figure 3**).

In addition, BCL family members (B-cell lymphoma-2 [Bcl2] and B-cell lymphoma-2-associated X [Bax]) and caspase proteins (caspase3 and cleaved caspase3) were further analyzed. The expression of Bax/Bcl2 and cleaved caspase3/caspase3 in the BCNC group was much higher than that in the control group. However, vacuum therapy decreased the expression of Bax/Bcl2 and cleaved caspase3/caspase3 (all *P* < 0.05), which suggested that vacuum therapy could downregulate apoptosis-related proteins and improve ED (**Figure 4**).

Vacuum therapy induced autophagy

TEM showed that compared with those of the control and therapy groups, pathological changes, such as mitochondrial turgescence,

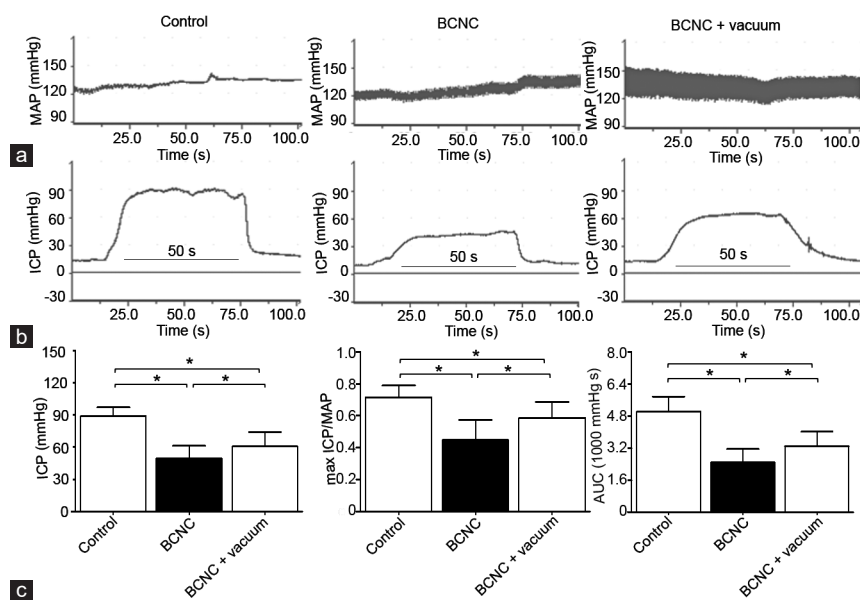


Figure 1: Vacuum therapy improved erectile dysfunction. Erectile function was evaluated by the max ICP, max ICP/MAP, and AUC in each group upon the same cavernous nerve electrical stimulation. Representative traces of (a) MAP and (b) ICP in the control, BCNC, and BCNC + vacuum groups. (c) The statistical analysis of max ICP, max ICP/MAP, and AUC in each group (*n* = 8). The data are expressed as the mean ± standard deviation. **P* < 0.05 indicates a significant difference between the two groups. AUC: area under the curve; BCNC: bilateral cavernous nerve crush; ICP: intracavernosal pressure; MAP: mean arterial blood pressure.

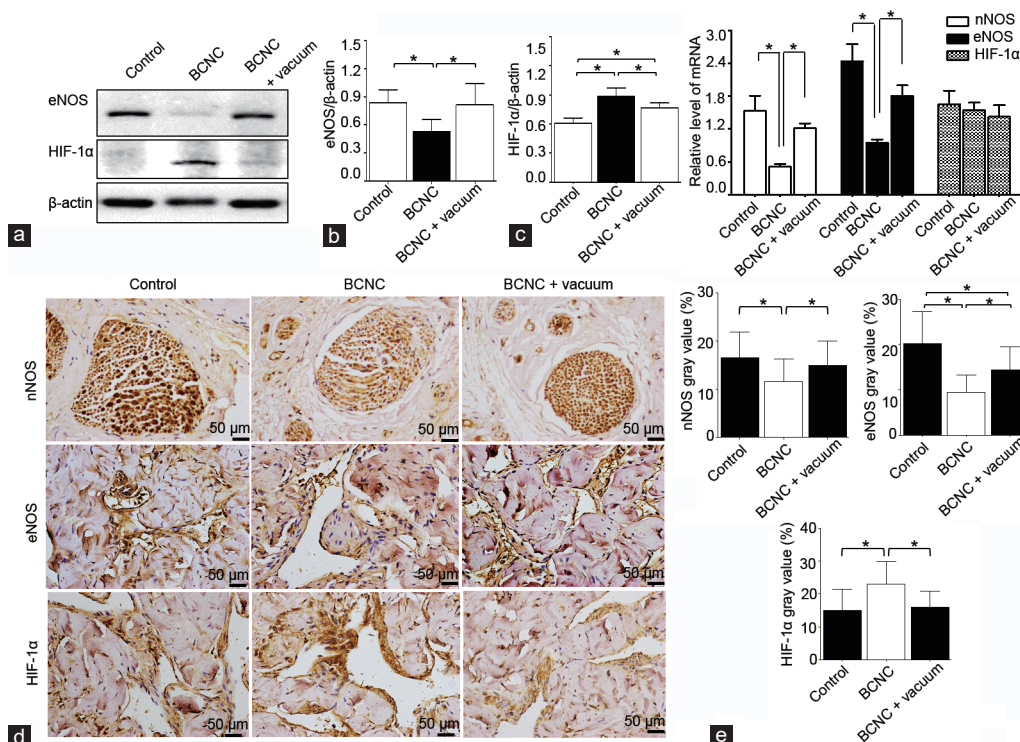


Figure 2: Vacuum therapy increased cavernosal oxygenation. (a) Representative WB protein bands of eNOS, HIF-1α, and β-actin and (b) the statistical analysis of the WB results ($n = 8$). (c) RT-qPCR was used to analyze the mRNA expression of nNOS, eNOS, and HIF-1α in each group ($n = 5$). (d) Representative immunohistochemistry images of nNOS, eNOS, and HIF-1α in each group; original magnification $\times 400$ (scale bars = 50 μm). (e) Statistical analysis of the immunohistochemistry results ($n = 5$). All data are expressed as the mean \pm standard deviation. * $P < 0.05$ indicates a significant difference between the two groups. BCNC: bilateral cavernous nerve crush; eNOS: endothelial nitric oxide synthase; HIF-1α: hypoxia-inducible factor-1 alpha; nNOS: neuronal nitric oxide synthase; RT-qPCR: real-time quantitative polymerase chain reaction; WB: western blot.

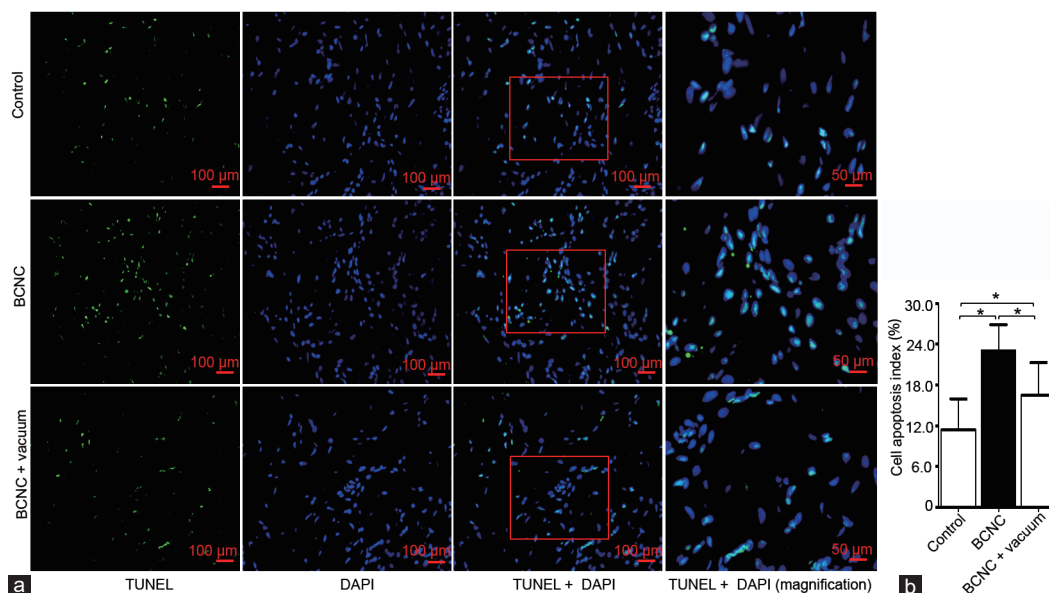


Figure 3: Vacuum therapy inhibited apoptosis. (a) TUNEL staining images of each group at $\times 200$ (scale bars = 100 μm) and $\times 400$ (scale bars = 50 μm) magnification. (b) The apoptotic index represents the percentage of apoptotic cells (green fluorescence) to total cells (blue fluorescence) within each section from each group of rats ($n = 5$). * $P < 0.05$ indicates a significant difference between the two groups. BCNC: bilateral cavernous nerve crush; TUNEL: TdT-mediated dUTP nick-end labeling; DAPI: 4',6'-diamidino-2-phenylindole.

endoplasmic reticulum distention, autophagosome deficiency, and endothelial dysfunction, were more serious in the BCNC group. These abnormalities were hypothesized to be associated with a prolonged absence of cavernosal oxygenation (Figure 5a).

To better understand the roles of autophagy in pPED and vacuum therapy, autophagy-related genes or proteins, including p62, Beclin1, and microtubule-associated protein 1 light chain 3B (LC3B)/microtubule-associated protein 1 light chain 3A (LC3A), were

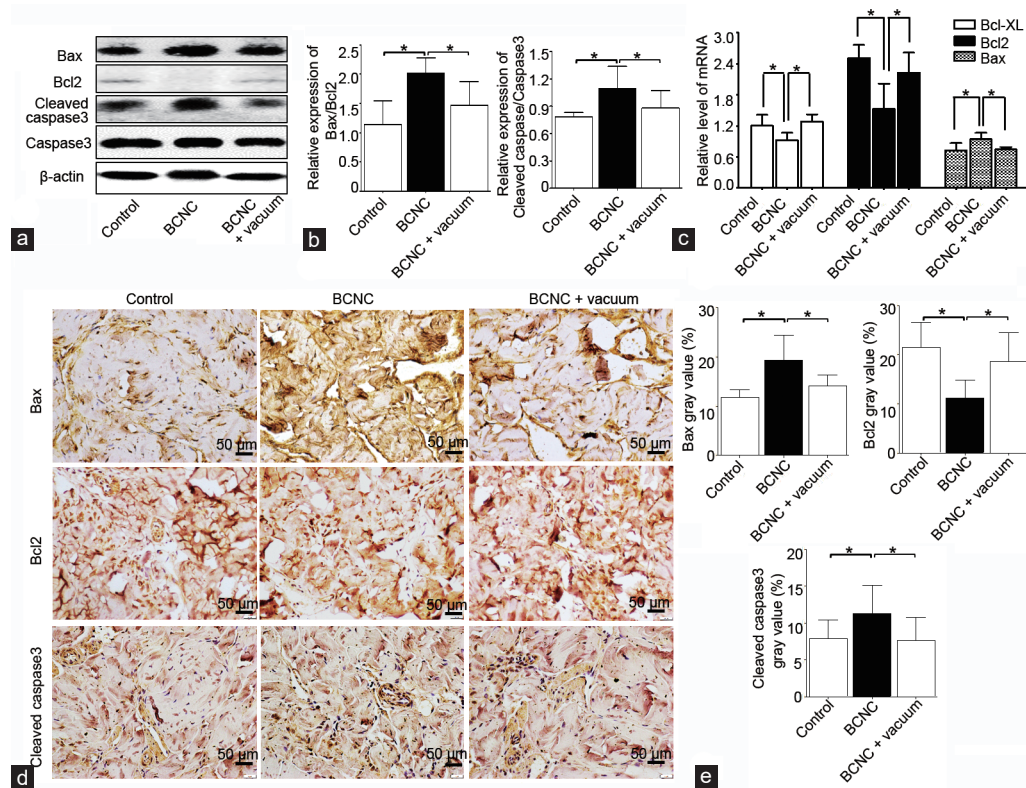


Figure 4: Vacuum therapy downregulated apoptosis-related proteins. (a) Representative WB bands of Bax, Bcl2, cleaved caspase3, caspase3, and β -actin and (b) the statistical analysis of Bax/Bcl2 and cleaved caspase3/caspase3 expression ($n = 8$). (c) Representative mRNA level of Bcl-XL, Bcl2, and Bax ($n = 5$). (d) Immunohistochemistry images of Bax, Bcl2, and cleaved caspase3 protein in each group, original magnification $\times 400$ (scale bars = 50 μm). (e) Statistical analysis of the immunohistochemistry results ($n = 5$). The data are expressed as the mean \pm standard deviation. * $P < 0.05$ indicates a significant difference between the two groups. Bax: BCL2-associated X; Bcl2: B-cell lymphoma-2; Bcl-XL: B-cell leukemia/lymphoma-xl; BCNC: bilateral cavernous nerve crush; WB: western blot.

measured. Compared with that of the control group and therapy group, the autophagy substrate p62 accumulated in the BCNC group ($P < 0.05$). Moreover, compared with the control and therapy groups, Beclin1 and LC3B/LC3A were significantly downregulated in the BCNC group (both $P < 0.05$). These results suggested that vacuum therapy improved ED by inducing autophagy (Figure 5b–5f).

Vacuum therapy activated autophagy via the phosphatidylinositol 3-kinase/AKT/mammalian target of rapamycin (PI3K/AKT/mTOR) signaling pathway

The PI3K/AKT/mTOR signaling pathway regulates autophagy by up- or downregulating unc-51-like autophagy-activating kinase 1 (ULK1) phosphorylation, which is responsible for autophagy initiation. In this study, the results showed that compared with those of the BCNC group, the expression of PI3K, phosphorylated AKT (pAKT)/AKT, phosphorylated mTOR (p-mTOR)/mTOR, and phosphorylated ULK1 (pULK1) (Ser757)/ULK1 was much lower in the control and therapy groups (all $P < 0.05$). These results revealed that vacuum therapy ameliorated ED through the PI3K/AKT/mTOR signaling pathway to induce autophagy (Figure 6).

DISCUSSION

According to previous research, there are mainly two types of pPED animal model: BCNC or bilateral cavernous nerve ablation (BCNA).^{14,29} Considering ICP tracing under cavernous nerve stimulation, BCNC rather than BCNA was selected for this study. After 4 weeks of vacuum therapy, ICP, max ICP/MAP, and AUC had increased in comparison

with those of the BCNC group. These outcomes agreed with those of our previous studies.³⁰ Further examination showed that vacuum therapy ameliorated cavernosal hypoxia by upregulating nNOS and eNOS expression and, as a result, decreased HIF-1 α levels. In addition, according to previous studies, apoptosis, especially that of cavernous smooth muscle cells, plays an important role in ED.¹⁷ Our results showed that the apoptosis index had significantly increased after cavernous nerves were injured. However, vacuum therapy not only decreased apoptosis but also induced autophagy by activating the PI3K/AKT/mTOR signaling pathway.

The loss of spontaneous erection and nocturnal tumescence resulting from cavernous nerve injury after RP is considered to be the initiating event for pPED. This subsequently leads to penile fibrosis and cavernous cell apoptosis due to cavernosal hypoxia. Therefore, a variety of therapeutic strategies, including vacuum therapy, are practiced to recover from cavernous nerve injury or increase NO production.^{31–34} NO is an important neurotransmitter that can mediate the NO/cGMP pathway, inducing smooth muscle relaxation and improving cavernosal hypoxia. In this study, after daily use of vacuum therapy on pPED, the expressions of nNOS and eNOS, two key enzymes associated with NO synthesis,^{35,36} had significantly upregulated in comparison with that of the BCNC group. In addition, HIF-1 α , an important oxygen sensor *in vivo* whose degradation depends on the oxygen concentration, had decreased after therapy. These outcomes suggested that vacuum therapy-mediated improvements in pPED were associated with increased cavernosal oxygen.

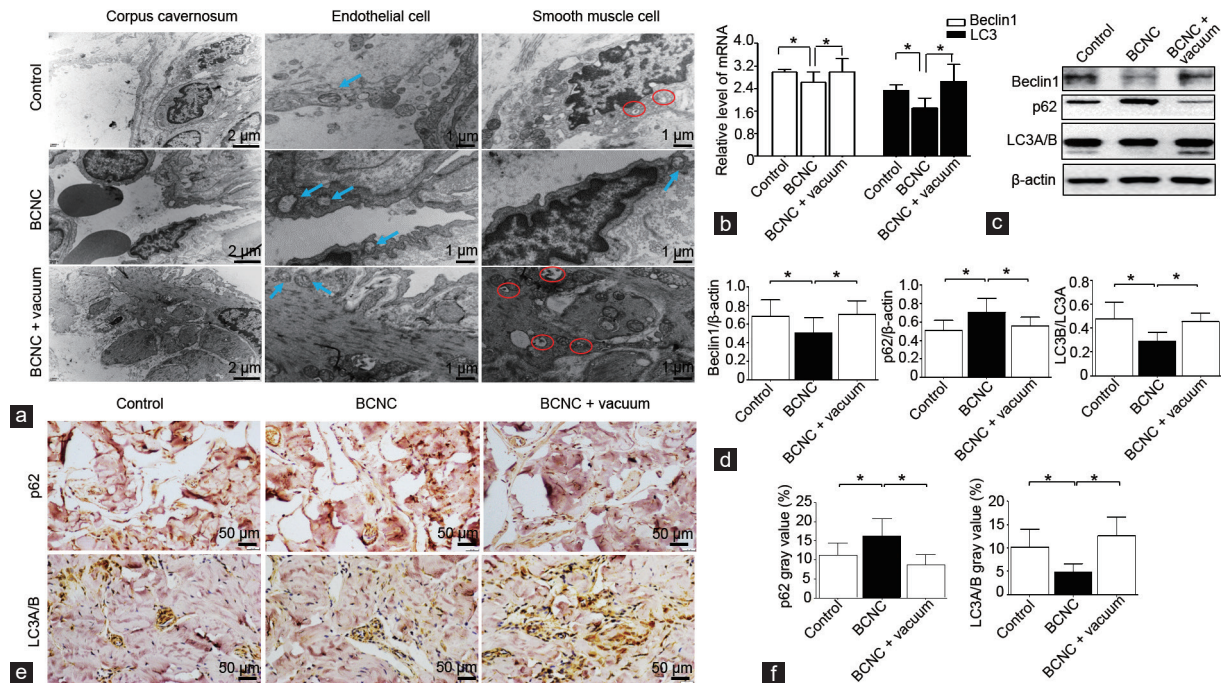


Figure 5: Vacuum therapy induced autophagy. (a) Electron microscopy was used to assess the autophagy level in each group at $\times 10\,000$ (scale bars = 2 μm) and $\times 12\,000$ (scale bars = 1 μm) magnification ($n = 3$). Mitochondria (blue arrow) and autophagosomes (red circle) were observed. (b) Representative mRNA level of Beclin1 and LC3 ($n = 5$). (c) Representative WB bands of the autophagy-related proteins such as Beclin1, p62, and LC3A/B and the reference protein β -actin. (d) Statistical analysis of Beclin1, p62, and LC3B/LC3A expression ($n = 8$). (e) Immunohistochemistry images of p62 and LC3A/B at $\times 400$ magnification (scale bars = 50 μm). (f) Statistical analysis of the immunohistochemistry results ($n = 5$). All data are expressed as the mean \pm standard deviation. * $P < 0.05$ indicates a significant difference between the two groups. BCNC: bilateral cavernous nerve crush; LC3: microtubule-associated protein 1 light chain 3; WB: western blot.

Apoptosis occurs extensively by activating an internally encoded suicide program, which refers to a cascade reaction of caspase proteins, cytochrome C, and calcium ions. Accumulating evidence has indicated that apoptosis, especially that of cavernosum smooth muscle cells, plays a crucial role in decreasing penile weight, veno-occlusive function, and ED.^{14,17} Moreover, in this study, TUNEL analysis showed that the apoptotic index in the BCNC group was much higher than that in the control group, and vacuum therapy inhibited apoptosis by downregulating apoptotic proteins. The relative expression of Bax/Bcl2 and cleaved caspase3/caspase3 in the therapy group had significantly decreased compared with that in the BCNC group. Furthermore, previous studies showed that decreased penile oxygen saturation resulting from denervation could lead to cell death.¹⁵ However, it is well known that vacuum therapy utilizes negative pressure to increase penile arterial inflow and improve cavernosal hypoxia. Therefore, inhibiting hypoxia might be the most direct antiapoptotic mechanism of vacuum therapy. In addition, our previous study also showed that oxidative stress was upregulated in pPED. Oxidative stress was also reported to induce apoptosis.³⁷ Thus, we hypothesized that antioxidative stress might be another mechanism by which vacuum therapy affects pPED. However, oxidative stress markers were not examined in this study.

Autophagy and apoptosis play important roles in maintaining intracellular homeostasis. Macroautophagy, ubiquitously referred to as autophagy, is so complex that it includes multiple phases, among which autophagosome formation is considered the most critical event. Therefore, observing autophagosomes by transmission electron microscopy is considered the gold standard to assess autophagic activity.³⁸ Our study showed that compared with that of the control

and vacuum therapy groups, the number of autophagosomes in corpus cavernosum cells had reduced in the BCNC group, whereas mitochondrial turgescence and endoplasmic reticulum distention were more severe. Based on the absence of a related reference on pPED and autophagy, we hypothesized that apoptosis might be more important than autophagy in prolonged hypoxia in the penis. In addition, the occurrence of autophagy depends on a series of proteins. The autophagic substrate p62 has negative autophagic activity.³⁹ Beclin1 and LC3A/B are essential molecules that mediate the elongation and completion of autophagosomes. Therefore, the expression of these proteins was a positive indicator of autophagic activity.^{30,41} In this study, the analysis of p62, Beclin1, and LC3B/LC3A revealed that autophagy was upregulated in the therapy group compared with that of the BCNC group. However, no significant difference was detected in the therapy and control groups, which might be related to mild autophagy being activated in normal penile tissue due to mild hypoxia.

Autophagy is regulated by many signaling pathways, such as 5'-adenosine monophosphate-activated protein kinase (AMPK)/mTOR, PI3K/AKT/mTOR, or mTOR (raptor)/p70S6K. However, almost all of these pathways eventually converge at the mTOR protein. mTOR is a key negative modulator of autophagy, whose activation phosphorylates downstream ULK1 to regulate autophagy.⁴² Some studies have indicated that the AMPK/mTOR and PI3K/AKT/mTOR signaling pathways play essential roles in pathological angiogenesis, such as in diabetic retinopathy or tumorigenesis. In fact, AMPK has a dual effect on angiogenesis. On the one hand, in metabolic syndrome, ischemia, or hypoxia, AMPK is activated, and mTOR is suppressed, inducing autophagy and stabilizing HIF-1 α . Furthermore, HIF-1 α , as a critical

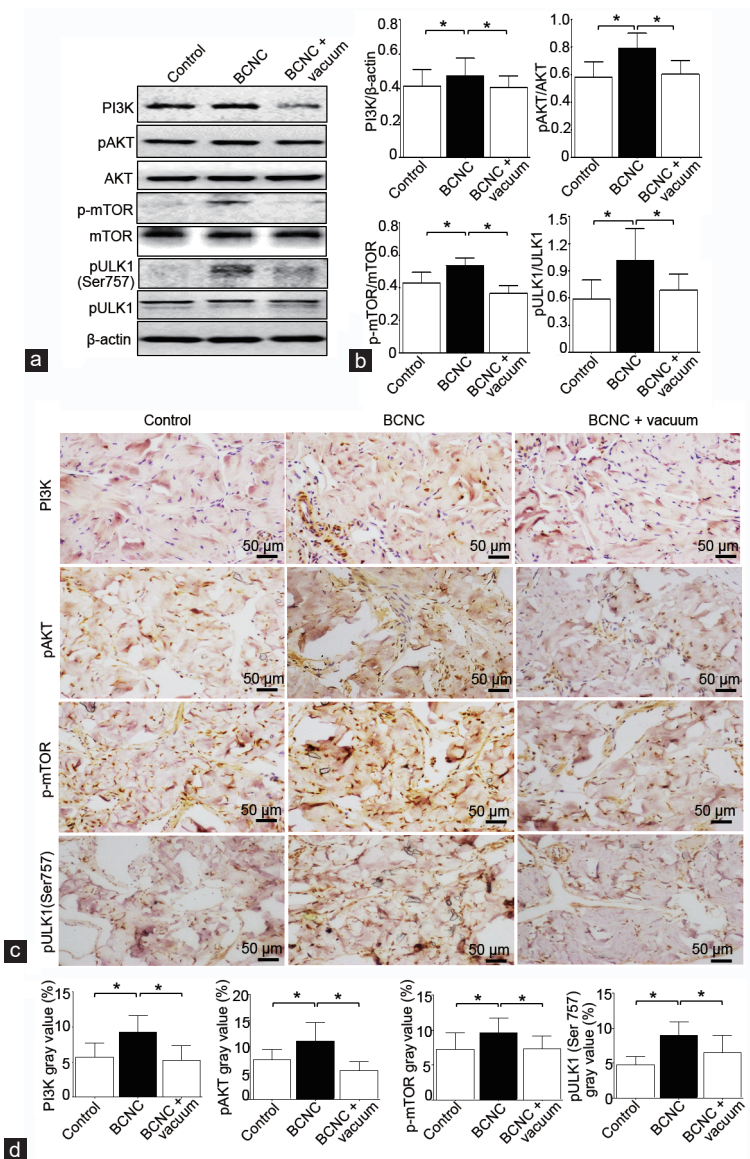


Figure 6: Vacuum therapy activated autophagy via the PI3K/AKT/mTOR signaling pathway. (a) Representative WB bands of PI3K, pAKT, AKT, pULK1 (Ser757), ULK1, p-mTOR, mTOR, and β -actin. (b) Statistical analysis of the WB results ($n = 8$). (c) Representative immunohistochemistry images of PI3K, pAKT, p-mTOR, and pULK1 (Ser757) at $\times 400$ magnification (scale bars = 50 μ m). (d) Statistical analysis of the immunohistochemistry results ($n = 5$). The data are expressed as the mean \pm standard deviation. * $P < 0.05$ indicates a significant difference between the two groups. AKT: protein kinase B (PKB); BCNC: bilateral cavernous nerve crush; p-mTOR: phosphorylated mammalian target of rapamycin; pULK1: phosphorylated unc-51-like autophagy-activating kinase; WB: western blot; PI3K: phosphatidylinositol 3-kinase.

transcriptional activator of vascular endothelial growth factor (VEGF), upregulates VEGF expression to promote angiogenesis.⁴³ On the other hand, AMPK can attenuate angiogenesis through the PI3K/AKT/mTOR pathway. Generally, PI3K/AKT is activated by mutations in PI3K or phosphatase and tensin homolog, the overexpression of growth factors, and cytokines. When PI3K/AKT is activated, mTOR is activated to increase HIF-1 α and VEGF.⁴⁴ In addition, it has been reported that the activation of PI3K/AKT may inhibit the tuberous sclerosis complex (TSC) by phosphorylating TSC2, which eventually activates mTOR.^{45,46} As noted above, mTOR is the key to multiple signaling pathways. In this study, we found that the mTOR and PI3K/AKT pathways were activated in the BCNC group, which might be associated with serious hypoxia because of denervation. When cavernosal hypoxia was improved by the therapy, mTOR and PI3K/AKT were downregulated, and autophagy

was induced. These findings revealed that the PI3K/AKT/mTOR signaling pathway mediated the effects of vacuum therapy on pPED by inhibiting apoptosis and activating autophagy. However, more detailed mechanisms need to be investigated in future.

CONCLUSIONS

In this study, autophagy was investigated for the first time in pPED and vacuum therapy. Vacuum therapy could ameliorate ED in bilateral cavernous nerve crush rats, and the mechanism may be related to inhibiting apoptosis and increasing autophagy.

AUTHOR CONTRIBUTIONS

CJW, FDF, MM, and XZY performed the experiments. CJW and FDF contributed to the statistical analysis and manuscript preparation. BTY, SZW, and FQ participated in the article screening and critical

revision of the manuscript. MM, CJW, FDF, and TL participated in the experimental design. JHY conceived this study, participated in its design and coordination, and helped draft the manuscript. All authors read and approved the final manuscript.

COMPETING INTERESTS

All authors declare no competing interests.

ACKNOWLEDGMENTS

This work was supported by the Natural Science Foundation of China (No. 81871147 and No. 82071639) and the Sichuan Science and Technology Program (No. 2018SZ0019 and No. 2018TJPT0018).

Supplementary Information is linked to the online version of the paper on the *Asian Journal of Andrology* website.

REFERENCES

- Walsh PC, Marschke P, Ricker D, Burnett AL. Patient reported urinary continence and sexual function after anatomic radical prostatectomy. *Urology* 2000; 55: 58–61.
- Salomon L, Anastasiadis AG, Katz R, de La Taille A, Saint F, *et al*. Urinary continence and erectile function: a prospective evaluation of functional results after radical laparoscopic prostatectomy. *Eur Urol* 2002; 42: 338–43.
- Giuliano F, Amar E, Chevallier D, Montaigne O, Joubert JM, *et al*. How urologists manage erectile dysfunction after radical prostatectomy: a national survey (repair) by the French urological association. *J Sex Med* 2008; 5: 448–57.
- Zagaja GP, Mhoon DA, Aikens JE, Brendler CB. Sildenafil in the treatment of erectile dysfunction after radical prostatectomy. *Urology* 2000; 56: 631–4.
- Montorsi F, Burnett AL. Erectile dysfunction after radical prostatectomy. *BJU Int* 2004; 93: 1–2.
- Montorsi F, Guazzoni G, Strambi LF, Da Pozzo LF, Nava L, *et al*. Recovery of spontaneous erectile function after nerve-sparing radical retropubic prostatectomy with and without early intracavernous injections of alprostadil: results of a prospective, randomized trial. *J Urol* 1997; 158: 1408–10.
- Weiss JN, Badlani GH, Ravalli R, Brettschneider N. Reasons for high drop-out rate with self-injection therapy for impotence. *Int J Impot Res* 1994; 6: 171–4.
- Köhler TS, Pedro R, Hendlin K, Utz W, Ugarte R, *et al*. A pilot study on the early use of the vacuum erection device after radical retropubic prostatectomy. *BJU Int* 2007; 100: 858–62.
- Nadig PW, Ware JC, Blumoff R. Noninvasive device to produce and maintain an erection-like state. *Urology* 1986; 27: 126–31.
- Raina R, Agarwal A, Ausmundson S, Lakin M, Nandipati KC, *et al*. Early use of vacuum constriction device following radical prostatectomy facilitates early sexual activity and potentially earlier return of erectile function. *Int J Impot Res* 2006; 18: 77–81.
- Yuan J, Lin H, Li P, Zhang R, Luo A, *et al*. Molecular mechanisms of vacuum therapy in penile rehabilitation: a novel animal study. *Eur Urol* 2010; 58: 773–80.
- Li E, Hou J, Li D, Wang Y, He J, *et al*. The mechanism of vacuum constriction devices in penile erection: the NO/cGMP signaling pathway. *Med Hypotheses* 2010; 75: 422–4.
- Lin HC, Yang WL, Zhang JL, Dai YT, Wang R. Penile rehabilitation with a vacuum erection device in an animal model is related to an antihypoxic mechanism: blood gas evidence. *Asian J Androl* 2013; 15: 387.
- Fall PA, Izicki M, Tu L, Swieb S, Giuliano F, *et al*. Apoptosis and effects of intracavernous bone marrow cell injection in a rat model of postprostatectomy erectile dysfunction. *Eur Urol* 2009; 56: 716–25.
- Klein LT, Miller MI, Buttyan R, Raffo AJ, Burchard M, *et al*. Apoptosis in the rat penis after penile denervation. *J Urol* 1997; 158: 626–30.
- Mulhall JP, Graydon RJ. The hemodynamics of erectile dysfunction following nerve-sparing radical retropubic prostatectomy. *Int J Impot Res* 1996; 8: 91–4.
- User HM, Hairston JH, Zelter DJ, McKenna KE, McVary KT. Penile weight and cell subtype specific changes in a post-radical prostatectomy model of erectile dysfunction. *J Urol* 2003; 169: 1175–9.
- Rabinowitz JD, White E. Autophagy and metabolism. *Science* 2010; 330: 1344–8.
- Lee IH, Kawai Y, Fergusson MM, Rovira II, Bishop AJ, *et al*. Atg7 modulates p53 activity to regulate cell cycle and survival during metabolic stress. *Science* 2012; 336: 225–8.
- Zhang KQ, Tian T, Hu LL, Wang HR, Fu Q. Effect of probucol on autophagy and apoptosis in the penile tissue of streptozotocin-induced diabetic rats. *Asian J Androl* 2020; 22: 409–13.
- Lin H, Wang T, Ruan Y, Liu K, Li H, *et al*. Rapamycin supplementation may ameliorate erectile function in rats with streptozotocin-induced type 1 diabetes by inducing autophagy and inhibiting apoptosis, endothelial dysfunction and corporal fibrosis. *J Sex Med* 2018; 15: 1246–59.
- Tang Z, Cui K, Luan Y, Ruan Y, Wang T, *et al*. Human tissue kallikrein 1 ameliorates erectile function via modulation of macroautophagy in aged transgenic rats. *Andrology* 2018; 6: 766–74.
- Wang XJ, Xu TY, Xia LL, Zhong S, Zhang XH, *et al*. Castration impairs erectile organ structure and function by inhibiting autophagy and promoting apoptosis of corpus cavernosum smooth muscle cells in rats. *Int Urol Nephrol* 2015; 47: 1105–15.
- Zhang J, Li AM, Liu BX, Han F, Liu F, *et al*. Effect of icaricide - on diabetic rats with erectile dysfunction and its potential mechanism via assessment of AGEs, autophagy, mTOR and the NO-cGMP pathway. *Asian J Androl* 2013; 15: 143–8.
- Zhu GQ, Jeon SH, Bae WJ, Choi SW, Jeong HC, *et al*. Efficient promotion of autophagy and angiogenesis using mesenchymal stem cell therapy enhanced by the low-energy shock waves in the treatment of erectile dysfunction. *Stem Cells Int* 2018; 8: 1–14.
- Lin H, Yuan J, Ruan KH, Yang W, Zhang J, *et al*. COX-2-10aa-PGIS gene therapy improves erectile function in rats after cavernous nerve injury. *J Sex Med* 2013; 10: 1476–87.
- Yang XL, Yang Y, Fu FD, Wu CJ, Qin F, *et al*. Optimal pressure in penile rehabilitation with a vacuum erection device: evidence based on a rat model. *Asian J Androl* 2019; 21: 516–21.
- Jaakkola P, Mole DR, Tian YM, Wilson MI, Gielbert J, *et al*. Targeting of HIF- α to the von Hippel-Lindau ubiquitylation complex by O₂-regulated prolyl hydroxylation. *Science* 2001; 292: 468–72.
- Mullerad M, Donohue JF, Li PS, Scardino PT, Mulhall JP. Functional sequelae of cavernous nerve injury in the rat: is there model dependency. *J Sex Med* 2006; 3: 77–83.
- Qian SQ, Qin F, Zhang S, Yang Y, Wei Q, *et al*. Vacuum therapy prevents corporeal veno-occlusive dysfunction and penile shrinkage in a cavernosal nerve injured rat model. *Asian J Androl* 2020; 22: 274–9.
- Dutta TC, Eid JF. Vacuum constriction devices for erectile dysfunction: a long-term, prospective study of patients with mild, moderate, and severe dysfunction. *Urology* 1999; 54: 891–3.
- Yuan J, Westney OL, Wang R. Design and application of a new rat-specific vacuum erection device for penile rehabilitation research. *J Sex Med* 2009; 6: 3247–53.
- Yuan J, Hoang AN, Romero CA, Lin H, Dai Y, *et al*. Vacuum therapy in erectile dysfunction-science and clinical evidence. *Int J Impot Res* 2010; 22: 211–9.
- Qian SQ, Gao L, Wei Q, Yuan J. Vacuum therapy in penile rehabilitation after radical prostatectomy: review of hemodynamic and antihypoxic evidence. *Asian J Androl* 2016; 18: 446–51.
- Burnett AL. Novel nitric oxide signaling mechanisms regulate the erectile response. *Int J Impot Res* 2004; 16: S15–9.
- Wessells H, Teal TH, Engel K, Sullivan CJ, Gallis B, *et al*. Fluid shear stress-induced nitric oxide production in human cavernosal endothelial cells: inhibition by hyperglycaemia. *BJU Int* 2006; 97: 1047–52.
- Modanloo M, Shokrzadeh M. Analyzing mitochondrial dysfunction, oxidative stress, and apoptosis: potential role of L-carnitine. *Iran J Kidney Dis* 2019; 13: 74–86.
- Ohsumi Y. Historical landmarks of autophagy research. *Cell Res* 2014; 24: 9–23.
- Itabura E, Mizushima N. p62 targeting to the autophagosome formation site requires self-oligomerization but not LC3 binding. *J Cell Biol* 2011; 192: 17–27.
- Tanida I, Minematsu-Ikeguchi N, Ueno T, Kominami E. Lysosomal turnover, but not a cellular level, of endogenous LC3 is a marker for autophagy. *Autophagy* 2005; 1: 84–91.
- Kadowaki M, Karim MR. Cytosolic LC3 ratio as a quantitative index of macroautophagy. *Methods Enzymol* 2009; 452: 199–213.
- Cudjoe EK Jr., Saleh T, Hawkridge AM, Gewirtz DA. Proteomics insights into autophagy. *Proteomics* 2017; 17: 1–17.
- Liang P, Jiang B, Li Y, Liu Z, Zhang P, *et al*. Autophagy promotes angiogenesis via AMPK/Akt/mTOR signaling during the recovery of heat-denatured endothelial cells. *Cell Death Dis* 2018; 9: 1152.
- Li Y, Sun R, Zou J, Ying Y, Luo Z. Dual roles of the AMP-activated protein kinase pathway in angiogenesis. *Cells* 2019; 8: 752–67.
- Laplante M, Sabatini DM. mTOR signaling at a glance. *J Cell Sci* 2009; 122: 3589–94.
- Corradetti MN, Inoki K, Bardeesy N, DePinho RA, Guan KL. Regulation of the TSC pathway by LKB1: evidence of a molecular link between tuberous sclerosis complex and Peutz-Jeghers syndrome. *Genes Dev* 2004; 18: 1533–8.

This is an open access journal, and articles are distributed under the terms of the Creative Commons Attribution-NonCommercial-ShareAlike 4.0 License, which allows others to remix, tweak, and build upon the work non-commercially, as long as appropriate credit is given and the new creations are licensed under the identical terms.

©The Author(s) (2021)



Supplementary Table 1: The primer sequences of real-time quantitative polymerase chain reaction

<i>Genes</i>	<i>Primer sequence (5'-3')</i>	<i>Genes</i>	<i>Primer sequence (5'-3')</i>
<i>nNOS</i>	F: CCTATGCCAAGACCCTGTGTGA R: CATTGCCAAAGGTGCTGGTG	<i>Bcl-XL</i>	F: AACTGGGGTCGATTGTG R: GATCCAAGGCTCTAGGTGGTC
<i>eNOS</i>	F: ACAGGCATCACCAGGAAGAAG R: CAGAGCCATACAGGATAGTCG	<i>Bcl-2</i>	F: TTGAGTTCGGTGGGGTCATG R: GATCCAGGTGTGAGATGCC
<i>HIF-1α</i>	F: TCAAGTCAGCAACGTGGAAG R: TTCACAAATCAGCACCAAGC	<i>Bax</i>	F: CCAAGAAGCTGAGCGAGTGTC R: TGAGGACTCCAGCCACAAAGA
<i>Beclin 1</i>	F: GGGCTCCTATTCCATCAAAA R: AACTGTGAGGACACCCAAGC	<i>β-actin</i>	F: AAGAGCTATGAGCTGCCTGA R: TACGGATGTCAACGTCACAC
<i>LC3</i>	F: CCAAGCCTTCTCCTCCTGG R: TCTCCTGGGAGGCATAGACC		

nNOS, neuronal nitric oxide synthesis; *eNOS*, endothelial nitric oxide synthesis; *HIF-1 α* , hypoxia-inducible factor 1 alpha; *LC3*, microtubule associated protein 1 light chain 3; *Bcl-XL*, B-cell leukemia/lymphoma-xl; *Bcl-2*, B-cell lymphoma-2; *Bax*, Bcl-2-associated X protein; F, forward; R, reverse.

Supplementary Table 2: Antibodies used in Western blot and immunohistochemistry

<i>Antibodies</i>	<i>WB</i>	<i>IHC</i>	<i>Product information</i>
HIF-1 α	1:1000	1:100	ab2185, Abcam, Cambridge, MA, USA
eNOS	1:1000	1:100	ab76198, Abcam
nNOS	---	1:100	Ab5586, Abcam
Bcl-2	1:800	1:80	AF6139, Affinity Bioscience, Wuhan, China
Bax	1:800	1:80	AF0120, Affinity Bioscience
Caspase3	1:1000	---	9662S, Cell Signaling Technology, Framingham, MA, USA
Cleaved-caspase3	1:800	1:80	AF7022, Affinity Bioscience
PI3K	1:1000	---	4255S, Cell Signaling Technology
AKT	1:1000	---	9272S, Cell Signaling Technology
Phospho-AKT	1:1000	---	9271S, Cell Signaling Technology
mTOR	1:1000	---	2983S, Cell Signaling Technology
Phospho-mTOR	1:1000	1:80	5536S, Cell Signaling Technology
ULK1	1:800	---	ET1704-63, HuaAn Biotechnology, Hangzhou, China
Phospho-ULK1	1:800	1:80	AF7022, Affinity Bioscience
Beclin1	1:1000	1:80	AF5128, Affinity Bioscience
p62	1:1000	1:80	AF5384, Affinity Bioscience
LC3A/B	1:1000	1:100	12741S, Cell Signaling Technology
β -actin	1:2000	---	M1210-2, HuaAn Biotechnology
Goat anti-rabbit IgG	1:10000	---	S0001, Affinity Bioscience
Goat anti-mouse IgG	1:10000	---	S0002, Affinity Bioscience

PI3K: phosphatidylinositol 3-kinase; mTOR: mammalian target of rapamycin; ULK1: unc-51-like autophagy-activating kinase 1; ---, no relevant measurement; WB: western blot; IHC: immunohistochemistry; HIF-1 α : hypoxia-inducible factor-1 α ; eNOS: endothelial nitric oxide synthesis; nnos: neuronal nitric oxide synthesis; Bcl-2: B-cell lymphoma-2; Bax: Bcl-2-associated X protein; AKT: protein kinase B.